Activity of Sub-Band Gap States in Ferroelectric Pb(Zr$_{0.2}$Ti$_{0.8}$)O$_3$ Thin Films

Niranjan Ramakrishnegowda, Yeseul Yun, David S. Knoche, Lutz Mühlenbein, Xinye Li, and Akash Bhatnagar*

Defect or intermediate states within the band gap of ferroelectric oxides are known to impact functional characteristics such as saturated polarization. However, depending upon their respective position, such levels can also induce a substantial photoelectrical response under appropriate illumination and severely impact the conduction mechanism of an otherwise highly insulating material system. Sub-band-gap illumination is used to highlight the activity of these levels in epitaxially grown and ferroelectric Pb(Zr$_{0.2}$Ti$_{0.8}$)O$_3$ thin films. Large transient effects are observed in relation to ferroelectric polarization and conductivity after illumination. In the case of polarization, light induces a "leaky" character, which eventually decays over a period of nearly 1.5 h. In conjunction, persistent photoconductivity is observed as the enhanced conductivity attained under illumination gradually decays over several minutes after removal of illumination. Thermally stimulated currents are measured to probe the presence of sub-band gap states and analyze their effect over a wide range of temperature. The trapping nature of the states and their role in the conduction is found to be the underlying origin.

1. Introduction

Pb(Zr$_x$Ti$_{1-x}$)O$_3$ is the most widely used piezoelectric and ferroelectric material with utility in a variety of applications such as sensors,[1] ferroelectric memories,[2] and piezoelectric actuators.[3] Photovoltaic effects have been also observed with origins attributed to either bulk photoeffects[4] or to the Schottky junction formed at the interface between the metal and ferroelectric.[5–7] Despite all the advances, there are certain issues related to functional properties that are not completely understood. For instance, a comprehensive understanding is still not available for issues pertaining to ferroelectric characteristics, such as fatigue, imprint, and retention. Fatigue has been extensively studied to be caused by domain wall pinning due to charge trapping effects at the defect sites,[8] which also includes the unavoidable interface between the conductive oxide and ferroelectric.[7] As a result, light of appropriate energy has been demonstrated to rejuvenate the sample as photo-excited carriers recombined with trapped charges.[7,9,10] Likewise, the origin of imprint, or the internal bias effect, has been proposed to be of electronic character.[11] Light-generated carriers can accumulate at domain walls which can stabilize one domain configuration over the other resulting in imprint effects.[12,13] This can also evidently affect the overall switchable polarization and cause degradation in charge retention over time.[14] Since the probable reasons for most of these phenomena are of electronic nature, light has been efficiently demonstrated as a diagnostic tool.[15] Above band-gap excitations are utilized to generate nonequilibrium carriers and the property of interest is monitored. Depending upon the role of the defect states, their subsequent neutralization causes an evident change in the value of the property under investigation. Interestingly, such defect states can also have a substantial impact on the photoelectrical properties. Persistent photoconductivity (PPC), that is, gradual decay of photoconductivity upon removal of illumination, has been mostly attributed to defect-mediated processes.[16,17] Photogenerated carriers trapped by such defects are slowly thermally released in the allowed bands which results in gradual decay of conductivity.

In this work, light of energy much below the reported band gap of Pb(Zr$_{0.2}$Ti$_{0.8}$)O$_3$ (PZT) has been used to emphasize upon the electronic contributions arising from levels or states within the band gap. First, a clear impact of light on the ferroelectricity is observed with polarization measurements before and after illumination. Subsequent to illumination, the well-saturated polarization gets massively overshadowed by leakage currents which gradually fade away with time, and polarization reverts back to initial value. Interestingly, conductivity in samples

N. Ramakrishnegowda, Y. Yun, D. S. Knoche, L. Mühlenbein, X. Li,
Dr. A. Bhatnagar
Zentrum für Innovationskompetenz SiLi-nano
06120, Halle (Saale), Germany
E-mail: akash.bhatnagar@physik.uni-halle.de
N. Ramakrishnegowda, Y. Yun, D. Knoche, L. Mühlenbein, X. Li,
Dr. A. Bhatnagar
Institute of Physics
Martin-Luther-Universität Halle-Wittenberg
06120, Halle (Saale), Germany

**ADVANCED
SCIENCE NEWS**
www.advancedsciencenews.com
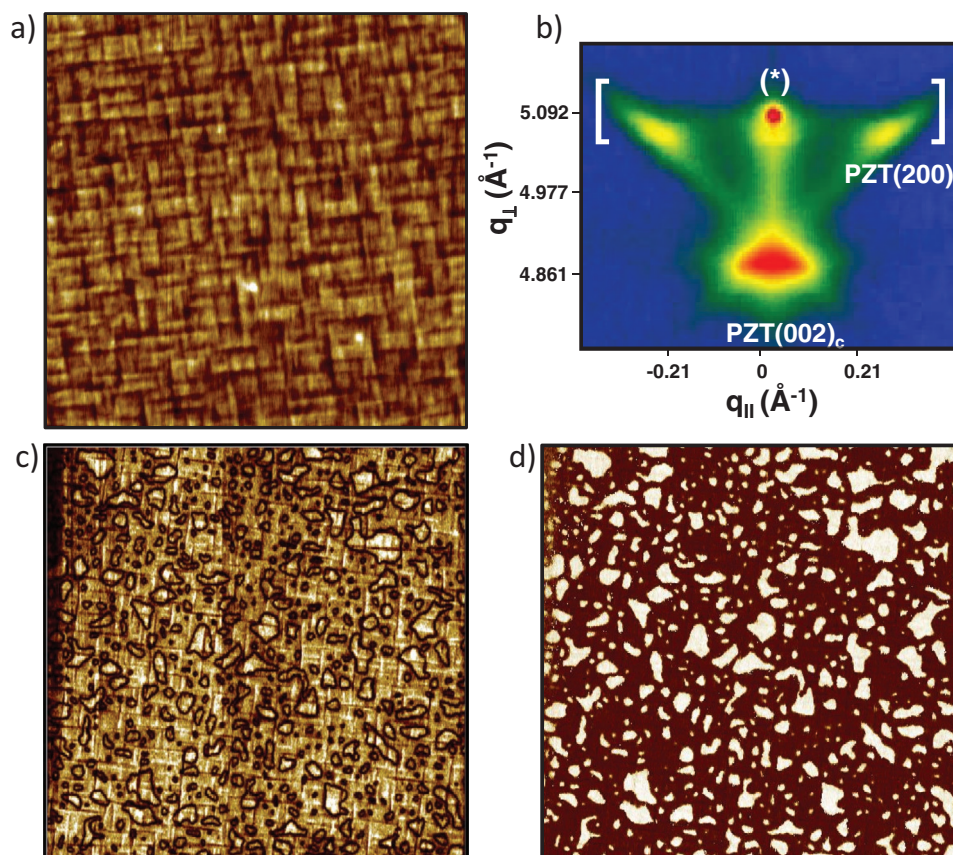
**ADVANCED
ELECTRONIC
MATERIALS**
www.advelectronicmat.de

Figure 1. a) Topography image of size 5×5 µm acquired from PZT/DSO thin film. b) RSM measured around $DSO(220)_o$ or $(002)_{pc}$. "*" indicates the reflection from the substrate and the squared brackets enclose the reflections arising from the *a*-domains. c,d) PFM images showing vertical amplitude and phase, respectively, acquired from the same area.

grown in identical conditions exhibits an analogous behavior. The higher photoconductivity measured during illumination steadily decayed in dark conditions over a long period of time. Both of these observations apparently imply substantial activity of levels within the band gap which were analyzed with thermally stimulated currents (TSC).

2. Results and Discussion

2.1. Thin Film Growth and Characterization

Thin films of PZT were fabricated on (110)-oriented $DyScO_3$ (DSO) substrates using a stoichiometric target. The electrical and photoelectrical measurements were conducted on PZT thin films deposited directly on the bare substrate, while for the ferroelectric characterization around 20 nm of $(La_{0.7}Sr_{0.3})MnO_3$ (LSMO) was deposited prior to PZT. **Figure 1**a,c,d show the images acquired with atomic- and piezo-force microscope (AFM and PFM) from sample PZT/DSO. A rich mixture of *a*- and *c*-domains is observed. The crosshatched stripe pattern which appears piezoelectrically inactive in the vertical amplitude response (Figure 1c) and topography (Figure 1a) is formed by the *a*-domains.[18] The region enclosed within and outside the crosshatched network constitutes of *c*-domains which are

polarized in up-and down-directions as visible in the out-of-plane phase image (Figure 1d).

Such an arrangement of *a*- and *c*-domains is known to occur in tetragonal ferroelectric films grown under in-plane anisotropic strain imposed by the substrate.[19–21] As the films are cooled through the Curie temperature, the nonequal lattice parameters of the substrate ($a = 3.9505$ Å, $b = 3.9468$ Å)[22] impose compressive strain of around 0.08% and 0.17% in (100) and (010) directions, respectively. Another reason for the polydomain configuration could be the large thickness of these PZT films (around 320 nm) which can trigger the release of mechanical and electrostatic stresses via domain formation.[23,24] This results in the formation of *a*1- and *a*2-domains with their respective polarization vectors perpendicular to one another. The presence of *a*-domains is also confirmed by the X-ray reciprocal space maps (RSM) acquired around $(002)_{pc}$ plane (Figure 1b).[25] Nevertheless, such a distribution of domains essentially makes the samples an ideal representation of PZT system.[26]

2.2. Ferroelectric Characterization

In **Figure 2**, the ferroelectric polarization (PV) and current–voltage (*I*–*V*) measurements conducted on the Au-Cr/PZT/LSMO/DSO sample are presented. Positive electric fields
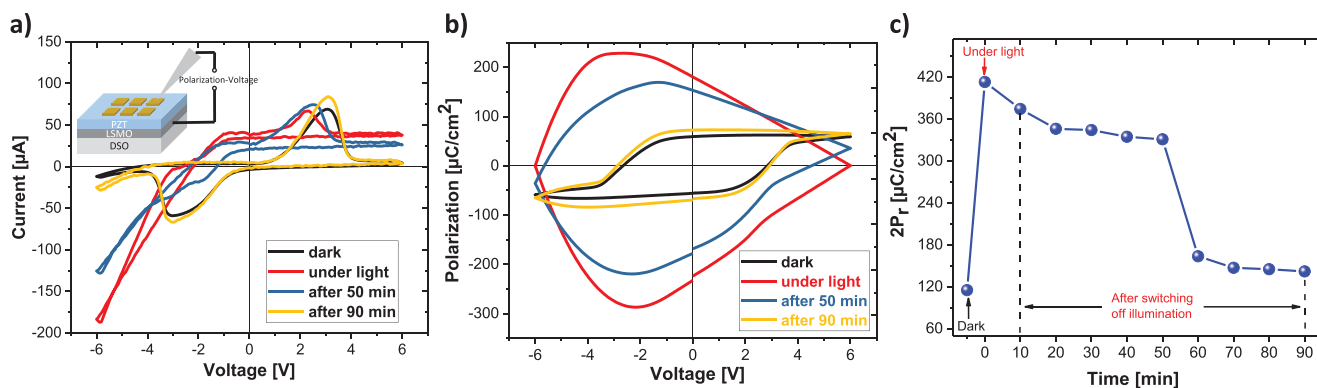
Figure 2. a,b) Ferroelectric switching characteristics, that is, current–voltage and polarization voltage measured in dark (black), under illumination (red), and after switching off the illumination (blue and yellow). Inset in (a) shows the measurement geometry. c) +2P_r values extracted from each PV loop plotted with the time interval. All the measurements presented in this figure were acquired from Au- Cr/PZT/LSMO/DSO sample.

result in distinct ferroelectric switching peaks with the current saturating for higher values of electric field (Figure 2a). Negative fields also result in clear ferroelectric switching albeit with contribution of leakage currents as the electric field increases. In these scenarios, the magnitude of the leakage current has been demonstrated to be affected by the rectifying quality of the diode formed between the metal–ferroelectric junction.[27,28] Thereafter, the polarization was measured under light of energy 3.06 eV (λ = 405 nm), which is around 0.54 to 0.4 eV below the reported band gap of PZT.[6,29] The PV measurement under light exhibits a substantial increment in the leakage current, as a result of which the polarization loop is also inflated (Figure 2b). Interestingly, a photovoltaic effect is also distinctly visible as the corresponding I–V curve undergoes an upward shift along the y-axis of current (Figure 2a, red line).

The illumination was then switched off and PV loops were acquired after every 10 min. In Figure 2a,b, loops measured after 50 and 90 min have been presented. It is evident from the measurement that the PV loop gradually relaxes back and becomes more saturated as a function of time. The sum of absolute remanent polarizations (+2P_r) was extracted from each PV loop to track the decay of leakage current and is presented in Figure 2c as a function of time. Interestingly, the eventual +2P_r at the end of 90 min is slightly higher than the initial +2P_r measured in dark conditions. Such enhancement of the polarization after light treatment has been investigated in PZT. The domains in PZT can be pinned by trapped charges which inhibit their reorientation under electric fields resulting in lower switchable polarization.[10,30] However, light-generated carriers can recombine with such trapped charges to unpin the domains and leading to higher values of +2P_r.[12] Its noteworthy to mention here that above band gap light was in used all such studies, wherein the generation can be attributed to band–band absorption. In this work we are using light of much lower energy which implies carrier generation from, or to sub-band gap states. Another issue of interest is the time-dependent decay of leakage currents which takes around 90 min. This evidently implies that the photo-generated carriers remain active for a certain period of time before eventually recombining.

2.3. Electrical Characterization

One of the consequences of such an extended life time of carriers can be PPC, defined as residual enhanced conductivity after illumination. The PPC effect has been observed in wide band gap insulators and oxide systems,[31–33] and can last from few hours to days. To investigate the validity of such a scenario, we used PZT films deposited on bare DSO substrates, grown under identical deposition conditions. Planar electrode geometries were utilized to manifest direct illumination of the film surface (**Figure 3**a). Likewise the PV measurements, light of wavelength 405 nm was used to illuminate the measurement gap at room temperature (RT). The current was recorded with a fixed bias voltage of 10 V. For the first 10 min, the current was recorded in the dark state with magnitude in the range of picoamperes. Thereafter, illumination was switched on for 10 min during which current in the range of microamperes was measured. The difference between the photoconductivities is around six orders of magnitude. Upon switching off the illumination, the current decays to much lower values over several thousands of seconds. Such a decay phenomenon can be analyzed with a mathematical relation of the type:[31,34,35]

$$I(t) = I_{01} \exp \frac{-t}{\tau_1} + I_{02} \exp \frac{-t}{\tau_2} \tag{1}$$

where $I(t)$ is the time (t) dependent decaying current and τ_1 and τ_2 are the decay times for the charge carriers. The fitting results in a quick τ_1 = 230 s and rather long τ_2 = 1.13 h. However, as visible in Figure 3a, the sample did not relax back to the initial dark state even after 90 min of measurements. In conjunction, I–V characteristics were measured in the dark state and 5 min after switching off the illumination (Figure 3b). Conduction mechanism in PZT, and in other ferroelectrics, with a certain distribution of trap level has been proven to be dominated by space charge limited currents[36–38] and the resultant current can be explained by the relation:

$$J = a\left(\frac{V}{d}\right) + b\left(\frac{V - V_o}{d}\right)^2 \tag{2}$$
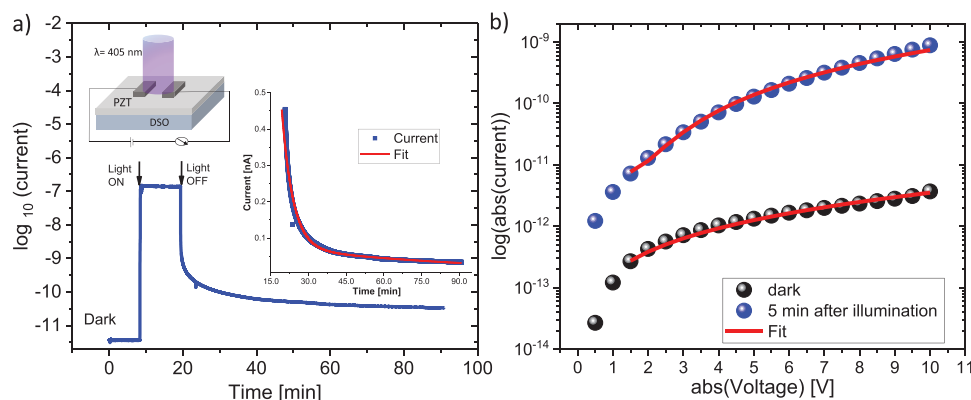
Figure 3. a) Current measured versus time with the sample initially in the dark state, followed by illumination for 10 min. The inset shows decay of current and the fit with Equation (1). b) Current versus voltage characteristics measured with the sample in the dark state (black) and 5 min after switching off the illumination (blue). The fit with Equation (2) is indicated with red line.

where a is the bulk property associated with Ohmic conduction, b is the space charge coefficient related to trap densities, V_o is the trapping potential of the levels, and d is the distance between the electrodes. Fitting the I–V characteristics with Equation (2) (Figure 3b) allowed us to extract the values of b which was around 1.72×10^{-14} Ω^{-1} V^{-1} in the dark state and 1.6×10^{-11} Ω^{-1} V^{-1} after illumination. The difference of three orders of magnitude can be attributed to the population of the trap levels with the photo-excited carriers and subsequent higher activity. From this analysis it becomes evident that the conduction mechanisms are heavily affected by sub-band gap levels which have a certain trapping character. However, it is still intriguing that such levels can be populated with light which is of much lower energy than the band gap. Some scenarios can be proposed in this regard. First, the carriers are excited directly to the level which is already in equilibrium with the allowed band at RT. As a result, carriers in these levels will have a finite probability to be re-emitted in the allowed band and contribute to conduction.[34,39] The eventual recombination process proceeds via this level resulting in longer lifetimes and PPC effect. In another scenario, a two-photon absorption can be perceived wherein the first process involves excitation of carriers to the levels while another photon is utilized to transfer the carriers to the allowed band. But, even in this case the level should remain in equilibrium with the allowed band. In the case of BiFeO3, such two-photon absorption has been confirmed with femtosecond absorption spectroscopy.[40] In either of these cases, light of energy below the band gap can be sufficient for causing enhanced conductivities.

2.4. Thermally Stimulated Currents

To further analyze the positions of these levels, we measured TSC. Similar measurements in the past have been demonstrated to be efficient in proving and estimating the activity of sub-band states in PbTiO3,[41] Pb(Zr,Ti)O3,[14] and BiFeO3.[31] In principle, such an analysis involves illuminating the sample at low temperature to fill the trapping levels, if there exists any, and then heating with a defined ramp rate.[42] The current

which is recorded during the ramping of temperature mostly constitutes of carriers freed from the levels, and can be represented by the following relation:[34,35,42]

$$J_{\text{TSC}} = J_{t0} \, P_t \exp\left(\frac{-1}{\gamma} \int P_t \, dt\right) \qquad (3)$$

where J_{t0} is the current arising from trap levels at 0 K, τ is the lifetime of the emitted carriers, γ is the heating rate, and P_t is the probability that trap carrier is emitted from the trap level. The probability is apparently temperature dependent and is given by:

$$P_t = N_c \, \beta_n \exp\left(\frac{-E_a}{kT}\right) \qquad (4)$$

where N_c represents the effective density of states, β_n is the capture coefficient of the trap level, and E_a is the activation energy of the trap. Also, it must be mentioned here that such relations are only valid for a single and discrete trap level.

We first conducted the TSC analysis by illuminating the sample for 10 min with 10 V bias at RT. Thereafter, the light was switched off and the sample was promptly quenched to 77 K. After settling down at low temperature, the temperature was ramped at 5 K min^{-1} to 400 K with continuous acquisition of current. **Figure 4**a shows the current response which exhibits a pronounced maximum. The response was analyzed with Equation (3) and evidently a good fit is obtained. The E_a was extracted to be around 0.30 eV with current peaking at 300.7 K. However, it is clear that conformity with Equation (3) gradually decreases after around 310 K as the peak decays. A probable reason could be the presence of another trap level which initiates to free up the carriers. To investigate this scenario, we conducted a TSC measurement wherein the sample was illuminated at 377 K instead of RT, with all the other parameters and protocol kept the same. The resultant TSC response (Figure 4b) exhibits a current peak at around 344 K which has an E_a of 0.41 eV. Also, the maximum current at the peak is much lower, that is 30 times, than in RT-illuminated TSC. Such an observation is understandable since at higher temperature (377 K), even deeper levels can be expected to be in equilibrium
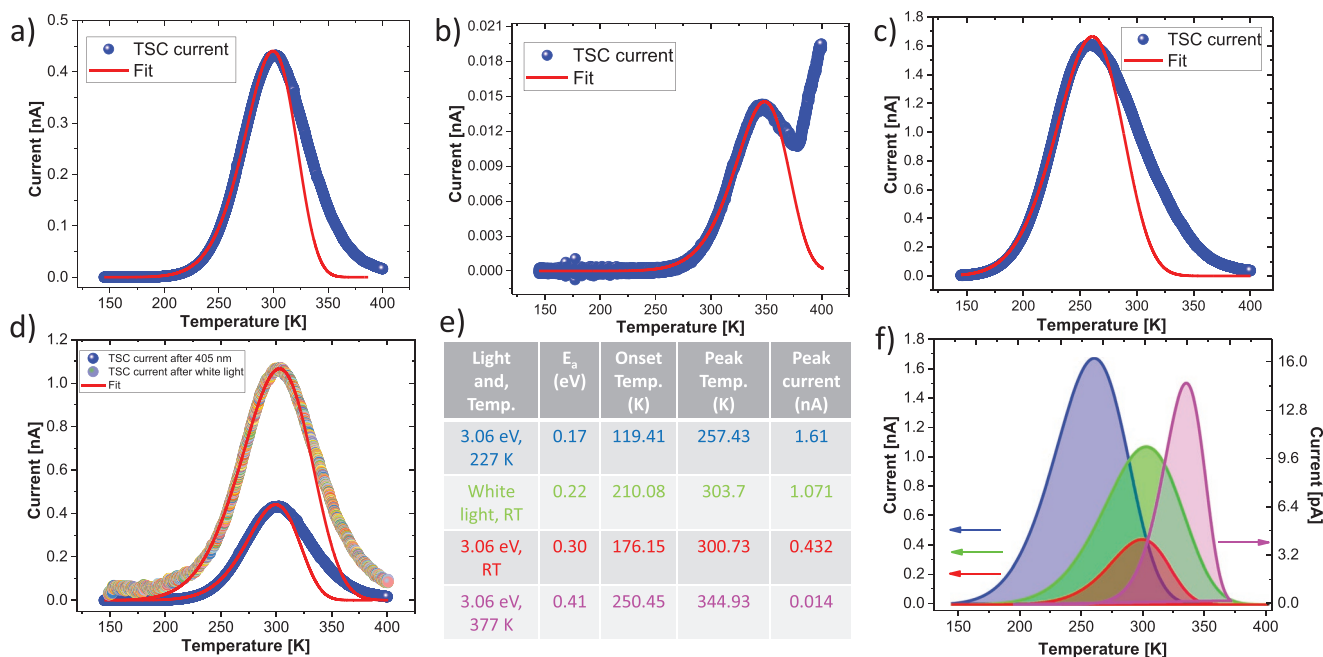
Figure 4. TSC measured after illuminating the sample with 405 nm light at: a) room temperature, b) 377 K, c) 227 K. d) TSC measured after illuminating with white light (multicolor) and 405 nm (blue, same curve as shown in [a]) at room temperature. The red line indicates the fit with Equation (3). In all the measurements presented here, a bias voltage of +10 V was continuously applied across the planar electrodes. e) Summary of different parameters extracted from each TSC measurement. f) Fits obtained from each TSC measurement presented in (a–d). The color scheme is the same as used in the table.

Light and, Temp.	E_a (eV)	Onset Temp. (K)	Peak Temp. (K)	Peak current (nA)
3.06 eV, 227 K	0.17	119.41	257.43	1.61
White light, RT	0.22	210.08	303.7	1.071
3.06 eV, RT	0.30	176.15	300.73	0.432
3.06 eV, 377 K	0.41	250.45	344.93	0.014

with the allowed bands, which apparently results in less trapping and lower values of maximum TSC. This was further proven when the sample was illuminated at 227 K followed by the TSC acquisition (Figure 4c). The TSC maximum is around four times higher than in Figure 4a and the corresponding E_a is around 0.17 eV. It is apparent from these results that the band gap of PZT is populated with levels which can be activated at appropriate temperatures upon excitation with sub-band gap light. Therefore, the TSC measurement conducted after illuminating with white light, instead of 405 nm, at RT resulted in a much higher current maximum albeit with slightly different E_a of 0.22 eV, Figure 4d.

In an attempt to assess the possible origin of such levels, we conducted measurements on a PZT/DSO sample grown in identical conditions but cooled in pO_2 = 50 mbar, instead of pO_2 = 600 mbar used previously. The RSM and PFM images acquired from sample are presented in Figure S1, Supporting Information. The apparent similarity between the samples in the context of domain arrangement is apparent. However, the acquired TSC upon subjecting the sample to identical duration of illumination and electric fields (as done for Figure 4a), does not reveal any peak-like feature, as evident from **Figure 5**. This apparently implies none or negligible activity of sub-band gap states within the investigated range of temperature. A possible scenario to explain the contrasting TSC responses from 50 and 600 mbar cooled samples involves the assumption that a certain number of Pb-based vacancies are created during the growth of the films.[43] Thereafter, in the case of 600 mbar cooled sample, these vacancies persist as the sample is cooled to room temperature. However, in the case 50 mbar cooled sample, these

vacancies are compensated by the oxygen vacancies[38] which are created during cooling. Similar treatment with reduced oxygen environment has been demonstrated to be critical in tuning the content of oxygen vacancies, and in turn tune the physical properties such as imprint,[44] fatigue,[45] and photoconductivity[46] in ferroelectrics. Thus, it can be implied that Pb vacancies have a dominant role in the appearance of peaks during the measurement of TSC and are potentially responsible for the observed sub-band gap related transient effects.
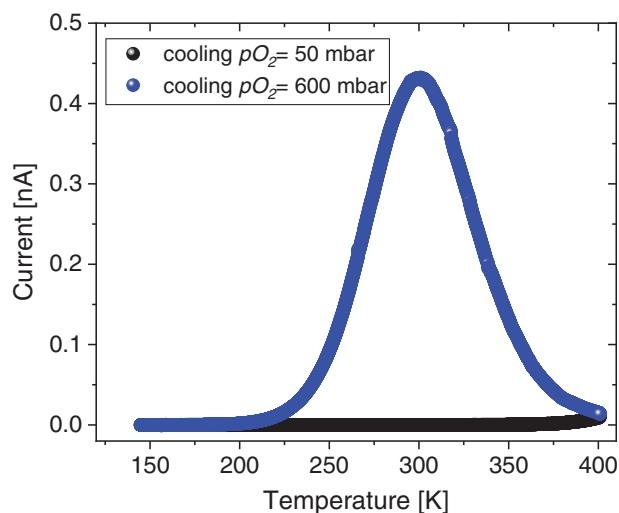

Figure 5. TSC measured from samples cooled with pO_2 = 600 mbar (same as Figure 4a) and 50 mbar.

ADVANCED
SCIENCE NEWS
www.advancedsciencenews.com

ADVANCED
ELECTRONIC
MATERIALS
www.advelectronicmat.de

3. Conclusions

With this knowledge in hand, we can now proceed to discuss the conduction mechanism in these PZT films. Initial measurements that were conducted in dark conditions results in saturated PV loops and Ohmic I–V characteristics. The transient effects pertaining to polarization relaxation and conductivity, that is, PPC effect, are observed only after exposure to light. The TSC analysis clearly demonstrates the presence of several levels which have temperature dependent trapping characters. Therefore, it can be assumed that most of the levels in the pristine samples are unoccupied. However, once the sample is exposed to illumination, the levels get populated with photo-excited carriers. As a result, they will have a higher probability to be remitted in the allowed band and contribute to conduction. The recombination process also is mediated via these levels and consequently is delayed. In ferroelectric characterization, the presence of these carriers manifests in higher leakage currents. The eventual recombination with trapped charges can unpin certain states of domains resulting in higher values of polarization. Time resolved analysis proved the delayed recombination with the observation of PPC and hours-long decay of conductivity. Analogous scenario results in dominant space-charge limited conduction in I–V characterization. Interestingly, the TSC also revealed the presence of other levels, and the associated thermal emptying of these levels extends well above room temperature. This is also evident from Figure 4f wherein, the fits obtained from all the measurements have been coplotted. All together, the investigated states can be expected to be active across a wide range of temperature from nearly 120 to 400 K, which can also be the operation temperature of many PZT-based devices. Therefore, the contribution of these levels to the room temperature transient effects cannot be neglected.

4. Experimental Section

Sample Fabrication: Samples were grown with pulsed laser deposition equipped with KrF excimer laser (248 nm). Homogenous termination at the surface of the substrates was achieved by annealing at 1000 °C for two hours. PZT was grown with a laser energy density of $\approx$1.4 J cm^{-2} with the substrate at 575 °C in an oxygen environment of 0.15 mbar. The samples were subsequently cooled in oxygen-rich conditions with around 600 mbar of oxygen partial pressure.

Ferroelectric Characterization: Layers of chromium and gold were deposited on the surface of PZT/LSMO/DSO sample using electron beam evaporation. The layers were deposited through a mask to form electrodes of size 50 µm by 50 µm. The PV loops were measured at a frequency of 2 kHz.

Electrical and Photoelectrical Characterization: Planar electrodes were fabricated with platinum using standard lithography and sputtering processes. The electrodes were 20 µm apart and $\approx$950 µm long. Photoelectrical measurements were conducted with laser illumination of wavelength 405 nm and 30 mW power. I–V characteristics were measured with high-impedance electrometer Keithley 6517B.

Supporting Information

Supporting Information is available from the Wiley Online Library or from the author.

Conflict of Interest

The authors declare no conflict of interest.

[1] P. Muralt, *IEEE Trans. Ultrason. Eng.* **2000**, *47*, 903.

[2] J. F. Scott, C. A. P. de Araujo, *Science* **1989**, *246*, 1400.

[3] H. Kueppers, T. Leuerer, U. Schnakenberg, W. Mokwa, M. Hoffmann, T. Schneller, U. Boettger, R. Waser, *Sens. Actuators, A* **2002**, *97-98*, 680.

[4] E. Dubovik, V. Fridkin, D. Dimos, *Integr. Ferroelectr.* **1995**, *8*, 285.

[5] V. K. Yarmarkin, B. M. Gol'tsman, M. M. Kazanin, V. V. Lemanov, *Phys. Solid State* **2000**, *42*, 522.

[6] L. Pintilie, I. Vrejoiu, G. Le Rhun, M. Alexe, *J. Appl. Phys.* **2007**, *101*, 064109.

[7] J. Y. Wang, G. Liu, D. Sando, V. Nagarajan, J. Seidel, *Appl. Phys. Lett.* **2017**, *111*, 092902.

[8] J. F. Scott, M. Dawber, *Appl. Phys. Lett.* **2000**, *76*, 3801.

[9] D. Dimos, H. N. Al-Shareef, W. L. Warren, B. A. Tuttle, *J. Appl. Phys.* **1996**, *80*, 1682.

[10] W. L. Warren, D. Dimos, B. A. Tuttle, R. D. Nasby, G. E. Pike, *Appl. Phys. Lett.* **1994**, *65*, 1018.

[11] M. B. Okatan, S. P. Alpay, *Appl. Phys. Lett.* **2009**, *95*, 092902.

[12] D. Dimos, W. L. Warren, M. B. Sinclair, B. A. Tuttle, R. W. Schwartz, *J. Appl. Phys.* **1994**, *76*, 4305.

[13] M. Grossmann, O. Lohse, D. Bolten, U. Boettger, T. Schneller, R. Waser, *J. Appl. Phys.* **2002**, *92*, 2680.

[14] H. Okino, Y. Toyoda, M. Shimizu, T. Horiuchi, T. Shiosaki, K. Matsushige, *Jpn. J. Appl. Phys.* **1998**, *37*, 5137.

[15] J. Lee, S. Esayan, A. Safari, R. Ramesh, *J. Appl. Phys.* **1995**, *6*, 289.

[16] B. A. Kulp, *J. Appl. Phys.* **1965**, *36*, 553.

[17] B. C. Burkey, R. P. Khosla, J. R. Fischer, D. L. Losee, *J. Appl. Phys.* **1976**, *47*, 1095.

[18] L. Feigl, P. Yudin, I. Stolichnov, T. Sluka, K. Shapovalov, M. Mtebwa, C. S. Sandu, X.-K. Wei, A. K. Tagantsev, N. Setter, *Nat. Commun.* **2014**, *5*, 4677.

[19] A. H. G. Vlooswijk, B. Noheda, G. Catalan, A. Janssens, B. Barcones, G. Rijnders, D. H. A. Blank, S. Venkatesan, B. Kooi, J. T. M. de Hosson, *Appl. Phys. Lett.* **2007**, *91*, 112901.

[20] O. Nesterov, S. Matzen, C. Magen, A. H. G. Vlooswijk, G. Catalan, B. Noheda, *Appl. Phys. Lett.* **2013**, *103*, 142901.

[21] N. A. Pertsev, A. G. Zembilgotov, *J. Appl. Phys.* **1996**, *80*, 6401.

[22] R. Uecker, B. Velickov, D. Klimm, R. Bertram, M. Bernhagen, M. Rabe, M. Albrecht, R. Fornari, D.G. Schlom, *J. Cryst. Growth* **2008**, *310*, 2649.

[23] V. Nagarajan, I. G. Jenkins, S. P. Alpay, H. Li, S. Aggarwal, L. Salamanca-Riba, A. L. Roytburd, R. Ramesh, *J. Appl. Phys.* **1999**, *86*, 595.

[24] V. Nagarajan, C. S. Ganpule, H. Li, L. Salamanca-Riba, A. L. Roytburd, E. D. Williams, R. Ramesh, *Appl. Phys. Lett.* **2001**, *79*, 2805.

[25] C. Hubault, C. Davoisne, L. Dupont, A. Perrin, A. Boulle, J. Holc, M. Kosec, M. G. Karkut, N. Lemée, *Appl. Phys. Lett.* **2011**, *99*, 052905.

[26] A. L. Roitburd, *Phys. Status Solidi A* **1976**, *37*, 329.

[27] L. Pintilie, I. Vrejoiu, D. Hesse, M. Alexe, *J. Appl. Phys.* **2008**, *104*, 114101.

[28] L. Pintilie, I. Vrejoiu, D. Hesse, G. LeRhun, M. Alexe, *Phys. Rev. B* **2007**, *75*, 63.

[29] J. Lee, S. Esayan, A. Safari, R. Ramesh, *Appl. Phys. Lett.* **1994**, *65*, 254.

[30] J.-L. Leray, O. Musseau, P. Paillet, J.-L. Autran, F. Sodi, Y.-M. Coic, *J. Phys. III* **1997**, *7*, 1227.

[31] A. Bhatnagar, Y. H. Kim, D. Hesse, M. Alexe, *Nano Lett.* **2014**, *14*, 5224.

[32] A. Tebano, E. Fabbri, D. Pergolesi, G. Balestrino, E. Traversa, *ACS Nano* **2012**, *6*, 1278.

[33] M. C. Tarun, F. A. Selim, M. D. McCluskey, *Phys. Rev. Lett.* **2013**, *111*, 187403.

[34] R. H. Bube, *Photoconductivity of Solids*, John Wiley & Sons, Inc., New York **1960**.

[35] R. H. Bube, *Photoelectronic Properties of Semiconductors*, 1st ed., Cambridge University Press, Cambridge **1992**.

[36] K. Watanabe, A. J. Hartmann, R. N. Lamb, J. F. Scott, *J. Appl. Phys.* **1998**, *21*, 241.

[37] B. M. Melnick, J. F. Scott, C. A. P. de Araujo, L. D. McMillan, *Ferroelectrics* **1992**, *135*, 163.

[38] J. F. Scott, C. A. Araujo, B. M. Melnick, L. D. McMillan, R. Zuleeg, *J. Appl. Phys.* **1991**, *70*, 382.

[39] *Thermally Stimulated Relaxation in Solids* (Ed: P. Bräunlich), Springer-Verlag, Berlin Heidelberg **1979**.

[40] E. Matsubara, T. Mochizuki, M. Nagai, T. Ito, M. Ashida, *Jpn. J. Appl. Phys.* **2015**, *54*, 092201.

[41] L. Pintilie, M. Alexe, I. Pintilie, I. Boierasu, *Ferroelectrics* **1997**, *201*, 217.

[42] G. A. Dussel, R. H. Bube, *Phys. Rev.* **1967**, *155*, 764.

[43] S. Pöykkö, D. J. Chadi, *Appl. Phys. Lett.* **2000**, *76*, 499.

[44] H.-S. Lee, K.-H. Auh, M.-S. Jeon, W.-S. Um, I.-S. Lee, G.-P. Choi, H.-G. Kim, *Jpn. J. Appl. Phys.* **1998**, *37*, 5630.

[45] D. J. Kim, T. S. Kim, J. K. Lee, H. J. Jung, *J. Mater. Res.* **1998**, *13*, 3442.

[46] R. L. Gao, H. W. Yang, C. L. Fu, W. Cai, G. Chen, X. L. Deng, J. R. Sun, Y. G. Zhao, B. G. Shen, *J. Alloys Compd.* **2015**, *624*, 1.